

Evolution of Cooperation on Stochastic Block Models

Babak Fotouhi^{1,2}, Naghmeh Momeni^{1,3}, Benjamin Allen^{1,4,5}, Martin A. Nowak^{1,6,7}

¹ Program for Evolutionary Dynamics, Harvard University, Cambridge, MA, USA

² Institute for Quantitative Social Sciences, Harvard University, Cambridge, MA, USA

³ Massachusetts Institute of Technology (MIT) - Sloan School of Management, Cambridge, MA, USA

⁴ Department of Mathematics, Emmanuel College, Boston, MA, USA

⁵ Center for Mathematical Sciences and Applications, Harvard University, Cambridge, MA, USA

⁶ Department of Mathematics, Harvard University, Cambridge, MA, USA

⁷ Department of Organismic and Evolutionary Biology, Harvard University, Cambridge, MA, USA

Cooperation is a major factor in the evolution of human societies. The structure of human social networks, which affects the dynamics of cooperation and other interpersonal phenomena, have common structural signatures. One of these signatures is the tendency to organize as groups. Among the generative models that network theorists use to emulate this feature is the Stochastic Block Model (SBM). In this paper, we study evolutionary game dynamics on SBM networks. Using a recently-discovered duality between evolutionary games and coalescing random walks, we obtain analytical conditions such that natural selection favors cooperation over defection. We calculate the transition point for each community to favor cooperation. We find that a critical inter-community link creation probability exists for given group density, such that the overall network supports cooperation even if individual communities inhibit it. As a byproduct, we present mean-field solutions for the critical benefit-to-cost ratio which performs with remarkable accuracy for diverse generative network models, including those with community structure and heavy-tailed degree distributions. We also demonstrate the generalizability of the results to arbitrary two-player games.

Cooperation is a central tenet of social life of many species. Cooperative dynamics are affected by the structure of social networks they take place on [1–4]. A ubiquitous feature of social networks, including human social networks, is community structure, which involves the tendency of nodes to have different intergroup and intragroup connectivity [5]. Previous studies have demonstrated the effects of such group structures. A common model to generate and study community structure and to perform community detection is the Stochastic Block Model (SBM) [6–8]. Here we study the evolutionary dynamics of arbitrary symmetric 2×2 games on SBM networks. We find analytical results such that natural selection would favor one strategy over the other. We introduce a mean-field approximation that produces remarkably-accurate solutions which perform reasonably well even when the network size is as small as 20. We utilize the solutions to study how inter-connection of segregated communities under the SBM framework affects the fate of cooperation in the whole network. We highlight that our results give analytical support to the previous studies in the literature which demonstrated the effect of inter-group connectivity on the evolution of cooperation with diverse simulation setups and model settings [9–12]. Together, these findings evince a robust phenomenon regarding how inter-group connectivity affects collective cooperation. We conclude by demonstrating that the proposed solutions perform remarkably well for network models other than SBM, including those with heavy-tailed degree distributions.

We consider a generic 2×2 game with two available

strategies, C and D. Both players receive R if they mutually play C, and receive P if they mutually play D. If one player plays C and the other plays D, the C-player receives S and the D-player receives T . The strategy of node x is denoted by $s_x \in \{0, 1\}$, where 1 corresponds to strategy C and 0 to strategy D. We denote the set of network neighbors of node x by \mathcal{N}_x . We consider averaged payoffs, where the payoff of node x is given by

$$f_x = \sum_{y \in \mathcal{N}_x} s_x [R s_y + S(1 - s_y)] + (1 - s_x) [T s_y + P(1 - s_y)]. \quad (1)$$

At each timestep, a random individual is chosen to update its strategy via copying that of a neighbor. The probability that neighbor x is copied is proportional to $1 + \delta f_x$, where f_x is the payoff of x and $0 < \delta \ll 1$ models the selection strength, that is, higher δ indicates stronger social learning via observing the payoff of peers. The case $\delta = 0$ is equivalent to the *voter model* [13–15]. The weak-selection limit considered here can be viewed as the first-order correction to the voter model. We seek an analytical condition such that natural selection favors the fixation of C over fixation of D. According to the Structure Coefficient Theorem [16], this happens if $(R - P)\sigma > (T - S)$, where σ is the structure coefficient, which is independent of the game and only depends on the network structure. Thus, it suffices to calculate σ for the given network. This can be done *exactly* by considering a mathematical equivalence between the evolutionary game dynamics and that of coalescing random walks [17]. Below we briefly outline this recent exact

framework, highlight the computational cost of the solution for very large networks, propose a mean-field approximation to ameliorate the situation for large networks, and then apply this mean-field solution to obtain remarkably accurate solutions for SBM networks. After analyzing the case of SBM networks in detail, we conclude by pointing out the reasonable performance of the proposed mean-field solution for a wide array of other network models.

To obtain σ for generic 2×2 games, we apply the methodology of [17] to unweighted undirected graphs. We analyze the ‘donation game’ version of the Prisoner’s Dilemma, with $R = b - 1$, $S = -1$, $T = b$, and $P = 0$ and later discuss how σ can be readily derived from the results. The payoff of node x is given by:

$$f_x(t) = -cs_x(t) + \frac{1}{k_x} \sum_{y \in \mathcal{N}_x} bs_y(t). \quad (2)$$

For the update of node x , the following holds:

$$\begin{aligned} \mathbb{E}[s_x(t+1)] &= (1 - \frac{1}{N})s_x(t) \\ &+ \frac{1}{N} \sum_{y \in \mathcal{N}_x} \frac{1 + \delta f_y(t)}{\sum_{z \in \mathcal{N}_x} [1 + \delta f_z(t)]} s_y(t). \end{aligned} \quad (3)$$

In the limit of weak selection, expanding to the first order of δ after multiplying both sides by k_x , we get:

$$\begin{aligned} \mathbb{E}[k_x s_x(t+1)] &= \frac{1}{N} \left[\sum_{y \in \mathcal{N}_x} s_y(t) + \delta \sum_{y \in \mathcal{N}_x} f_y(t) s_y(t) \right. \\ &\left. - \sum_{y, z \in \mathcal{N}_x} \delta \frac{s_y(t) f_z(t)}{k_x} \right] + O(\delta^2) + (1 - \frac{1}{N})k_x s_x(t). \end{aligned} \quad (4)$$

Now we define $\psi(t) := \sum_x k_x s_x(t)$. Summing (4) over all nodes, we see that in the zeroth-order dynamics of the system (i.e., $\delta = 0$, corresponding to the voter model), the expected value of $\psi(t)$ is a conserved quantity [13, 15, 18]. The fixation probability can be obtained by equating the average value of ψ over every initial mutant placement with its expected value as $t \rightarrow \infty$. The expected first-order change of ψ is

$$\begin{aligned} \Delta\psi^{(1)}(\vec{s}) &= \frac{\delta}{N} \left[\sum_x \sum_{y \in \mathcal{N}_x} f_y s_y - \sum_x \sum_{y, z \in \mathcal{N}_x} \frac{s_y f_z}{k_x} \right] \\ &= \frac{\delta}{N} \left[\sum_x k_x f_x s_x - \sum_x \sum_{y, z \in \mathcal{N}_x} \frac{s_y f_z}{k_x} \right] \\ &= \frac{\delta}{N} \sum_x \left[k_x s_x \left(-cs_x + \frac{b}{k_x} \sum_{y \in \mathcal{N}_x} s_y \right) \right. \\ &\left. - \sum_{y, z \in \mathcal{N}_x} \frac{s_y \left(-cs_z + \frac{b}{k_z} \sum_{w \in \mathcal{N}_z} s_w \right)}{k_x} \right] \end{aligned} \quad (5)$$

Exchanging the summation order, denoting the first moment of the degree distribution (the average degree) by μ_1 , we get

$$\begin{aligned} \Delta\psi^{(1)}(\vec{s}) &= -\frac{\delta}{N} c(N\mu_1) + \frac{\delta}{N} \sum_y \left[b \sum_{x \in \mathcal{N}_y} s_y s_x \right. \\ &\left. + c \sum_{x \in \mathcal{N}_y} \sum_{z \in \mathcal{N}_x} \frac{s_y s_z}{k_x} - b \sum_{x \in \mathcal{N}_y} \sum_{z \in \mathcal{N}_x} \sum_{w \in \mathcal{N}_z} \frac{s_y s_w}{k_x k_z} \right]. \end{aligned} \quad (6)$$

We need to sum up these expected increments from $t = 0$ up to $t = \infty$. Let ξ_x denote this expected total change for given initial condition in which only node x is C and all other nodes are D. The fixation probability for a given initial condition will then be $(k_x + \xi_x)/(N\mu_1)$. Averaging over all nodes, this becomes:

$$\rho = \frac{1}{N} + \frac{1}{N} \sum_x \xi_x. \quad (7)$$

The sum on the right hand side of (7) requires the calculation of temporal sum of the spin products on the right hand side of (6). Note that these summations are to be performed in the voter-model regime. That is, due to the factor δ , we should only keep the summations in zeroth order. In [17, 19], it is shown that for any two nodes i and j , if we find the expected temporal sum of $1/N - s_i s_j$ from $t = 0$ to $t = \infty$ under the voter-model dynamics and then average this sum over all single-node initial placements, the result is equal to $\tau_{ij}/(2N)$, where τ_{ij} is the expected meeting time of two random walkers initiated at nodes i and j . These meeting times follow the following recurrence relation:

$$\tau_{ij} = \tau_{ji} = (1 - \delta_{ij}) \left[1 + \frac{1}{2k_i} \sum_{\ell \in \mathcal{N}_i} \tau_{\ell j} + \frac{1}{2k_j} \sum_{\ell \in \mathcal{N}_j} \tau_{i \ell} \right]. \quad (8)$$

Thus the random walk equivalence relates the fixation probability to the expected value of the meeting times of two random walkers initiated one, two, and three steps away on the network, corresponding to the three last terms on the right hand side of Equation (6), respectively. Note that the expression ‘ ℓ steps away’ here refers to random-walk steps, rather than graph distance. So for example, node y is ℓ steps away from node x if $A_{xy}^\ell > 0$, where A^ℓ is the ℓ -th power of the adjacency matrix. Using the meeting times which are the solutions to the system of equations (8), we define the quantity τ_x as the expected remeeting time of two random walkers both initiated at node x :

$$\tau_x = 1 + \frac{1}{k_x} \sum_{y \in \mathcal{N}_x} \tau_{yx}. \quad (9)$$

We also define $p_x = \sum_{y \in \mathcal{N}_x} 1/(k_x k_y)$. Using these definitions, and after some algebraic simplifications, the fixation probability can be expressed in the following form:

$$\rho = \frac{1}{N} + \frac{\delta}{2N} \left[b \left(\sum_x \frac{k_x}{N\mu_1} \tau_x - 2 \right) - c \left(\sum_x \frac{k_x}{N\mu_1} \tau_x p_x - 2 \right) \right] + O(\delta^2). \quad (10)$$

The critical benefit-to-cost ratio for C to be favored by natural selection is thus given by setting this fixation probability be greater than neutral drift, which yields:

$$b^* = \frac{\sum_x \tau_x k_x - 2N\mu_1}{\sum_x \tau_x k_x p_x - 2N\mu_1}. \quad (11)$$

The drawback of this exact framework is that solving (8) requires solving a system of $N(N-1)/2$ linear equations, which can be infeasible for very large networks. The conventional Cholesky decomposition methods to solve this system have the complexity of order N^6 , and faster techniques are mainly applicable only when the network is sparse. So for large networks in general, which can as well be dense, obtaining the exact solution is computationally infeasible. To obviate this limitation, here we seek a mean-field approximation to obtain analytical results that are computationally feasible for large networks. We use the fact that, combining (9) and (8), the remeeting times of these random walkers satisfy the following equation:

$$\sum_x k_x^2 \tau_x = N^2 \mu_1^2. \quad (12)$$

Using this equation and assuming a mean-field approximation in which every τ_x value is replaced by the average value over all x , we get:

$$\tau_x = N \frac{\mu_1^2}{\mu_2}, \quad (13)$$

where μ_2 is the second moment of the degree distribution. For the mean-field approximation of the fixation probability, we plug this into (10) and obtain:

$$\rho \approx \frac{1}{N} + \frac{\delta}{2N} \left[b \left(N \frac{\mu_1^2}{\mu_2} - 2 \right) - c \left(\frac{\mu_1}{\mu_2} \sum_x k_x p_x - 2 \right) \right] \quad (14)$$

Noting that $\sum_x k_x p_x = \sum_x \sum_{y \in \mathcal{N}_x} 1/k_y$ is equal to N for any network, we get:

$$\rho \approx \frac{1}{N} + \frac{\delta}{2N} \left[b \left(N \frac{\mu_1^2}{\mu_2} - 2 \right) - c \left(\frac{N\mu_1}{\mu_2} - 2 \right) \right] \quad (15)$$

Plugging this result into (11), we arrive at:

$$b^* \approx \frac{N - 2 \frac{\mu_2}{\mu_1^2}}{\frac{N}{\mu_1} - 2 \frac{\mu_2}{\mu_1^2}} \quad (16)$$

We consider a stochastic block model [6, 7] with m equi-probable groups, intra-community link probability p and inter-community link probability q . For node x with degree k_x , denote the number of within-community neighbors by k_x^{intra} and denote the number of its neighbors in other communities by k_x^{inter} . For large N , the average degree μ_1 , which is the expected value of k_x , is

$$\mu_1 = \mathbb{E}(k_x^{\text{intra}}) + \mathbb{E}(k_x^{\text{inter}}) = p \frac{N-1}{m} + q(N-1) \left(1 - \frac{1}{m} \right). \quad (17)$$

Also because the inter and intra-community degree distributions are independent, the variance of k is the sum of the variance of k_x^{intra} and the variance of k_x^{inter} :

$$\text{var}(k) = p(1-p) \frac{N-1}{m} + q(1-q)(N-1) \left(1 - \frac{1}{m} \right). \quad (18)$$

Combining (17) and (18), we obtain μ_2 , which we can insert into (15) to obtain the fixation probability. For the critical benefit-to-cost ratio, we insert the expression for μ_2 and μ_1 into (16). Defining $\alpha := 1/m$ and $\beta := 1 - 1/m$ for brevity, and after algebraic simplifications, we obtain:

$$b_{\text{SBM}}^* \approx \frac{N - 2 - \frac{2}{N-1} \frac{\alpha p(1-p) + \beta q(1-q)}{(\alpha p + \beta q)^2}}{\frac{N/(N-1)}{\alpha p + \beta q} - 2 - \frac{2}{N-1} \frac{\alpha p(1-p) + \beta q(1-q)}{(\alpha p + \beta q)^2}}. \quad (19)$$

Figure 1 demonstrates that the approximation (19) has relative error less than 1% for network size as small as 40. In these network sizes, the exact method can be employed in reasonable time and thereby we have a benchmark to assess the solutions. Figure 1 demonstrates that for large networks, the error rate is remarkably small, so for large networks where the exact method become prohibitively constly

The special case of $p = q$ is equivalent to the Erdős-Rényi (ER) model [20]. Equivalently, we can set $m = 1$. In this special case Equation (19) simplifies to:

$$b_{\text{ER}}^* \approx \frac{p(N^2 - 3N + 4) - 2}{(N-2)(1-2p)}. \quad (20)$$

Figure 2 illustrates the accuracy of the proposed mean-field approximation (20) for ER networks. We plot $1/b^*$

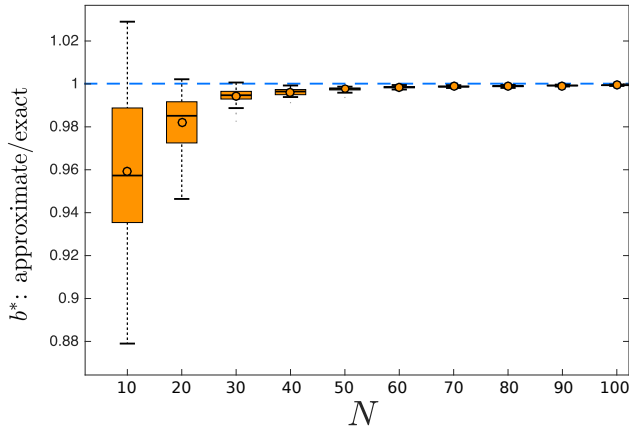


FIG. 1. (Color Online) Accuracy of the proposed mean-field approximation for b^* as a function of N . The network generation parameters are set to the example values of $p = 0.7$, $q = 0.1$, and $m = 3$. The performance is consistently well for every parameter configuration tried, which will be demonstrated in Figure 4.

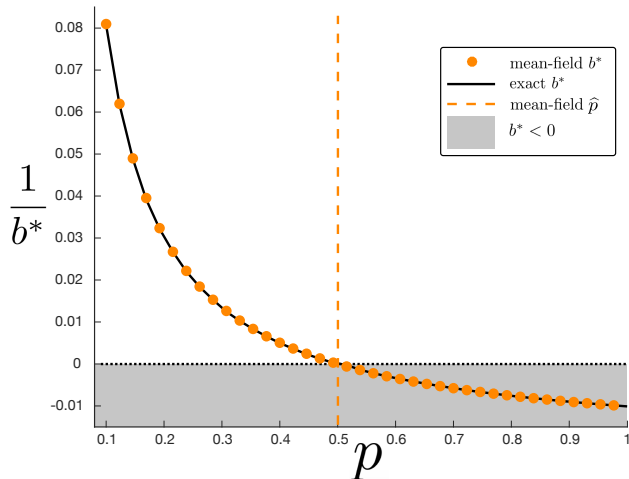


FIG. 2. (Color Online) Accuracy of the proposed mean-field approximation for b^* for ER networks as a function of link creation probability p . As predicted by Equation (20), there is a phase transition at $\hat{p} = 1/2$, above which natural selection does not favor cooperation over defection regardless of the benefit-to-cost ratio. The mean-field prediction is in agreement with the exact results.

instead of b^* because it gives visually better results. Equation (20) indicates a phase transition at $\hat{p} = 1/2$, which is visible in Figure 2. That is, in the ER model, the expected value of the critical benefit-to-cost ratio becomes negative if $p > \hat{p}$. In this regime, the fixation probability of a cooperative mutant is less than that of neutral drift, regardless of the values of b and c . Hence natural selection does not favor the fixation of cooperation over the fixation of defection for *any* value of benefit-to-cost ratio. In this regime, the network promotes spite, which means that players are willing to pay a cost to reduce the payoff of others. Hence we observe

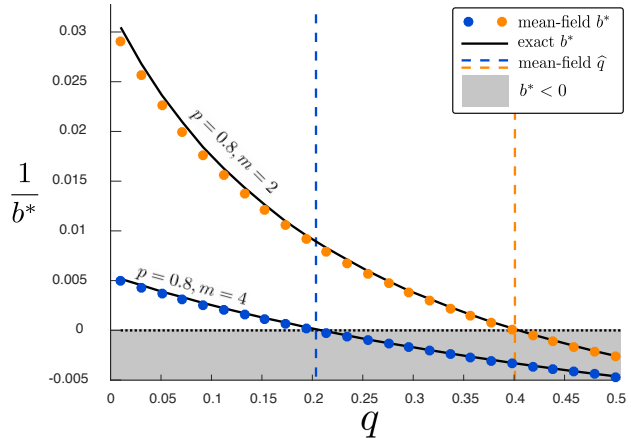


FIG. 3. (Color Online) Accuracy of the proposed mean-field approximation for b^* for the example value of $p = 0.8$, and two different values of m . The network size is 100. The dashed lines depict the predicted threshold value \hat{q} as given by (21), agrees with the exact results for both settings. For $q > \hat{q}$, natural selection promotes fixation of defection over cooperation regardless of the benefit-to-cost ratio. The intercepts match the result for $\lim q \rightarrow 0^+$ obtained in Equation (22).

a phase transition from cooperation to spite governed by network density.

For the general case of $p \neq q$, too, we can find such a point of transition. We can find \hat{q} (the critical inter-community link probability above which natural selection does not favor fixation of cooperative mutants over defective mutants regardless of the benefit-to-cost ratio) by setting the denominator of Equation (19) equal to zero and solving the resulting quadratic equation for q . Expanding the solution for large N , we get:

$$\hat{q} = \frac{m - 2p}{2(m - 1)} + 2m \frac{(\frac{1}{2} - p)^2}{(m - 1)^2} \frac{1}{N} + O\left(\frac{1}{N^2}\right). \quad (21)$$

This result has an important consequence. Each of the m communities with intra-community link probability p considered separately is an ER network, so the expected value of the critical benefit-to-cost ratio for each of them is given by (20). Suppose the communities have $p > 1/2$, which, as discussed above, means that cooperation is not favored by natural selection for each individual community considered separately. We can then interconnect these communities under the SBM setting, with inter-community probability q . For $q < \hat{q}$, the critical benefit-to-cost ratio of the overall network is positive, despite individual communities inhibiting the fixation of cooperation. This confirms analytically the numerical observations about conjoining random networks [21].

In Figure 3, we present the comparison of Equation (19) with the exact results. The orange markers pertain to the example case of $m = 4$ and $p = 0.8$, for which Equation (21) gives $\hat{q} \approx 0.4$. The blue markers

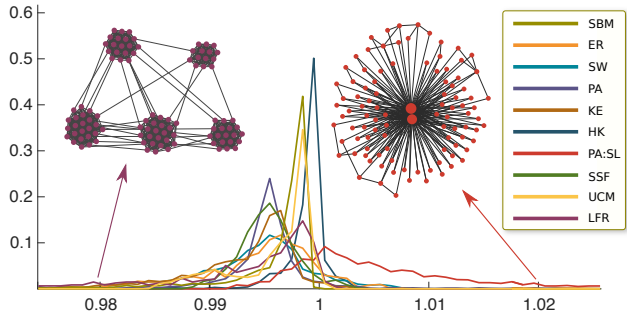


FIG. 4. (Color Online) The distribution of the ratio of the proposed mean-field approximation to the true value of b^* . The true value is obtained by solving the $N(N-1)/2$ linear equations as given by (8), which is infeasible for very large networks, but feasible for the size ranges of the test networks. The 10 network generation families are discussed in the text. Two example graphs with high heterogeneity are depicted to highlight the robustness of the proposed mean-field approximation to structural heterogeneity.

pertain to $m = 2$ and $p = 0.8$, with $\hat{q} \approx 0.2$. The network size is 100 in both cases. The approximations are remarkably close to the exact values.

Of particular relevance for actual scenarios is the case where $q \ll 1$, which means that the communities are sparsely interconnected. In this regime, we can expand b^* as follows:

$$b^* = \frac{N(N-2)p - 2m(1-p)}{N(m-2p) - 2m(1-p)} + O(q). \quad (22)$$

The interesting result here is the existence of the zeroth-order term. This fact can be seen in Figure 3 as well. For $N = 100, p = 0.8$ with $m = 2$, from Equation (22) we get $b^* \approx 200$, and with $m = 4$ we get $b^* \approx 32.9$. The inverse of these values are 0.0050 and 0.030, respectively, which correctly match the intercepts observed in Figure 3. This confirms that in the limit as $q \rightarrow 0^+$, b^* tends to a positive number. Thus, sparse interconnection of cohesive communities rescues cooperation. Note that this happens as long as the whole network is connected, so that b^* is well-defined. The minimum value of q such that the whole network is connected goes to zero as N tends to infinity.

Returning to arbitrary 2×2 games, according to the Structure Coefficient Theorem, the structure coefficient is defined in terms of b^* as follows:

$$\sigma = \frac{b^* + 1}{b^* - 1}. \quad (23)$$

For the special case of SBM or ER networks, σ can be obtained readily by inserting the corresponding values of b^* from Equations (19) and (20) into (23), respectively. For general networks, we use the mean-field value for b^* obtained in (16). The result simplifies to the following:

$$\sigma \approx \frac{N(\mu_1 + 1) - 4\mu_2/\mu_1}{N(\mu_1 - 1)}. \quad (24)$$

Natural selection favors the fixation of strategy C over the fixation of strategy D if $(R-P)\sigma > (T-S)$. Thus we have obtained analytical conditions such that natural selection favors the fixation of one strategy over the other for any 2×2 game.

We conclude by highlighting the accuracy of the proposed mean-field approximation for b^* via simulations and numerical results for various graph families, in addition to the SBM and ER models. In Figure 4, we plot the histogram of the ratio of the approximate b^* to the exact value (computed via solving the system of $N(N-1)/2$ linear equations as given by (8)) for 10 different network families. In addition to SBM and ER networks, we consider the Small-world model, and 7 other network generation families, which all generate networks with heavy-tailed degree distribution. We use these additional 7 families as pessimistic scenarios regarding our mean-field approximation, because these models generate highly-heterogeneous networks. For the SBM model, we chose m uniformly from $\{2, 3, 4, 5\}$, chose p uniformly in $[0.1, 1]$, and q uniformly in $[.01, p]$. For the small-world model [22], we chose the initial lattice degree uniformly from $\times\{4, 8, 12\}$ and the link creation probability uniformly from $[0, 0.1]$. For ER networks, we chose the link formation probability uniformly in $[0.2, 1]$. For preferential attachment (PA) with shifted-linear kernel [23] (also called ‘initial attractiveness’), we randomly generate m between 1 and 5, and the kernel bias is generated randomly between 0 and 5 (the closer to zero, the closer the model is to the Barabasi-Albert model). For the scale-free model of Holme and Kim (HK) [24], we chose the triad formation probability of the model uniformly in $[0, 1]$. For Klemm-Euigluz (KE) scale-free model [25], we choose the cross-over probability parameter of the model uniformly in $[0, 1]$. For both models, we choose the number of initial connections of incoming nodes uniformly between 1 and 5. For the spatial scale-free model of Barthelemy [26] (SSL), we generated networks on a 2D lattice with distance decay parameter r_c chosen uniformly in $[0, 0.2]$. For the uncorrelated configuration model (UCM) [27], we chose the minimum number of connections uniformly between 1 and 5, and the exponent in the power-law degree distribution is chosen uniformly in $[1, 4]$. For super-linear preferential attachment [28] (PA:SL), where the attachment kernel depends on degrees as k^θ , we chose the number of initial connections of incoming nodes uniformly between 1 and 4, and the exponent of the kernel uniformly in $[0, 3]$. Greater exponents produce networks with higher degree inequality. The LFR benchmarks [29] are generated with the mixing parameter chosen uniformly at random in $[0, 1]$. The maximum degree k_{\max} was chosen uniformly between 1 and $N-1$, the average degree was chosen uniformly between 1 and k_{\max} , the degree exponent was uniformly in $[0, 3]$, the exponent for the community size distribution

was chosen uniformly in $[0, 1]$. For each family, we generate 10000 networks. For every generate network, the size is randomly chosen between 100 and 500, which is reasonably small so that the exact results could be feasibly calculated via solving Equation (8). The histograms are highly concentrated around unity, which confirms the accuracy of the proposed mean-field approximations. Interestingly, the proposed approximation works well for networks with high structural heterogeneity, including those with heavy-tailed degree distributions.

We presented accurate mean-field solutions for 2×2 games on heterogeneous networks that determine which strategy is favored by natural selection. We have utilized our solution to study the case of SBM networks in detail, and have uncovered a network-structural phase transition which pertains to regions in which one of the strategies will not be favored by natural selection regardless of the payoff parameters. We have obtained similar results for ER networks as a special case. We have obtained analytical expressions for the inter-connection of segregated communities, which individually inhibit cooperation, but after interconnection, can collectively favor cooperation. This result in agreement with the previous results in the literature [9, 11], which obtain qualitatively similar results via various updating schemes and simulation parameters, and even those that consider many-player games [10]. Our analytical findings together with the previous simulation studies consistently highlight the cooperative advantage of sparsely interconnecting cohesive communities, and indicate that this advantage is a robust feature of cooperative dynamics on networks, which has notable real-world consequences.

-
- [1] E. Lieberman, C. Hauert, and M. A. Nowak, *Nature* **433**, 312 (2005).
- [2] G. Szabó and G. Fath, *Physics reports* **446**, 97 (2007).
- [3] M. Perc, J. Gómez-Gardeñes, A. Szolnoki, L. M. Floría, and Y. Moreno, *Journal of the royal society interface* **10**, 20120997 (2013).
- [4] M. Perc and A. Szolnoki, *BioSystems* **99**, 109 (2010).
- [5] M. Girvan and M. E. Newman, *Proceedings of the national academy of sciences* **99**, 7821 (2002).
- [6] P. W. Holland, K. B. Laskey, and S. Leinhardt, *Social networks* **5**, 109 (1983).
- [7] A. Decelle, F. Krzakala, C. Moore, and L. Zdeborová, *Physical Review E* **84**, 066106 (2011).
- [8] B. Karrer and M. E. Newman, *Physical review E* **83**, 016107 (2011).
- [9] Z. Wang, A. Szolnoki, and M. Perc, *Scientific reports* **3**, 2470 (2013).
- [10] Z. Wang, A. Szolnoki, and M. Perc, *Scientific reports* **3**, 1183 (2013).
- [11] L.-L. Jiang and M. Perc, *Scientific reports* **3**, 2483 (2013).
- [12] Z. Wang, A. Szolnoki, and M. Perc, *Journal of theoretical biology* **349**, 50 (2014).
- [13] V. Sood and S. Redner, *Physical review letters* **94**, 178701 (2005).
- [14] T. Antal, S. Redner, and V. Sood, *Physical review letters* **96**, 188104 (2006).
- [15] V. Sood, T. Antal, and S. Redner, *Physical Review E* **77**, 041121 (2008).
- [16] C. E. Tarnita, H. Ohtsuki, T. Antal, F. Fu, and M. A. Nowak, *Journal of theoretical biology* **259**, 570 (2009).
- [17] B. Allen, G. Lippner, Y.-T. Chen, B. Fotouhi, N. Momeni, S.-T. Yau, and M. A. Nowak, *Nature* **544**, 227 (2017).
- [18] B. Fotouhi and M. G. Rabbat, *The European Physical Journal B* **87**, 55 (2014).
- [19] Y.-T. Chen *et al.*, *The Annals of Applied Probability* **23**, 637 (2013).
- [20] P. Erdős and A. Rényi, *Publicationes Mathematicae* **6**, 290 (1959).
- [21] B. Fotouhi, N. Momeni, B. Allen, and M. A. Nowak, *arXiv preprint arXiv:1805.12215* (2018).
- [22] M. E. Newman and D. J. Watts, *Physics Letters A* **263**, 341 (1999).
- [23] S. N. Dorogovtsev, J. F. F. Mendes, and A. N. Samukhin, *Physical review letters* **85**, 4633 (2000).
- [24] P. Holme and B. J. Kim, *Physical review E* **65**, 026107 (2002).
- [25] K. Klemm and V. M. Eguiluz, *Physical Review E* **65**, 057102 (2002).
- [26] M. Barthélemy, *EPL (Europhysics Letters)* **63**, 915 (2003).
- [27] M. Catanzaro, M. Boguná, and R. Pastor-Satorras, *Physical Review E* **71**, 027103 (2005).
- [28] P. L. Krapivsky, S. Redner, and F. Leyvraz, *Physical review letters* **85**, 4629 (2000).
- [29] A. Lancichinetti, S. Fortunato, and F. Radicchi, *Physical review E* **78**, 046110 (2008).